

# Disparity of superconducting and pseudogap scales in low- $T_c$ Bi-2201 cuprates

Th. Jacobs,<sup>1</sup> S. O. Katterwe,<sup>1</sup> H. Motzkau,<sup>1</sup> A. Rydh,<sup>1</sup> A. Maljuk,<sup>2</sup>  
T. Helm,<sup>3</sup> C. Putzke,<sup>4</sup> E. Kampert,<sup>5</sup> M. V. Kartsovnik<sup>3</sup>, and V. M. Krasnov<sup>1\*</sup>

<sup>1</sup>*Department of Physics, Stockholm University, AlbaNova University Center, SE-10691 Stockholm, Sweden*

<sup>2</sup>*Leibniz Institute for Solid State and Materials Research IFW Dresden, Helmholtzstr. 20, D-01171 Dresden, Germany*

<sup>3</sup>*Walther-Meissner-Institut, Bayerische Akademie der Wissenschaften,*

*Walther-Meissner-Str. 8, D-85748, Garching, Germany*

<sup>4</sup>*H. H. Wills Physics Laboratory, University of Bristol,*

*Tyndall Avenue, Bristol, BS8 1TL, United Kingdom*

<sup>5</sup>*Helmholtz-Zentrum Dresden-Rossendorf, Hochfeld-Magnetlabor Dresden, DE-01314 Dresden, Germany*

(Dated: March 1, 2012)

We experimentally study transport and intrinsic tunneling characteristics of a single-layer cuprate  $\text{Bi}_{2+x}\text{Sr}_{2-y}\text{CuO}_{6+\delta}$  with a low superconducting critical temperature  $T_c \lesssim 4$  K. It is observed that the superconducting energy, critical field and fluctuation temperature range are scaling down with  $T_c$ , while the corresponding pseudogap characteristics have the same order of magnitude as for high- $T_c$  cuprates with 20 to 30 times higher  $T_c$ . The observed disparity of the superconducting and pseudogap scales clearly reveals their different origins.

PACS numbers: 74.72.Gh 74.55.+v 74.72.Kf 74.62.-c

An interplay between the normal state pseudogap (PG) and unconventional superconductivity remains one of the highly debated and controversial issues. For high transition temperature cuprates the energy scales of the superconducting gap (SG) and the PG are similar ( $\sim 30$ – $50$  meV). They are close to several oxygen phonon modes and comparable to the antiferromagnetic exchange energy. It remains unsettled whether this is a mere coincidence, a prerequisite for a high  $T_c$ , or an indication of the common origin of the SG and the PG. Within the precursor superconductivity scenario of the PG, the apparent large difference between the PG suppression temperature  $T^*$  and  $T_c$  is attributed to large phase fluctuations (for review, see e.g. Ref. [1]). The extent of fluctuations is determined by the ratio of the superconducting energy gap  $\Delta_{\text{SG}}$  to the Fermi energy  $E_F$  and the dimensionality of the system [1]. Therefore, it is instructive to compare superconducting and PG characteristics of homologous series of cuprates with different number of CuO planes per unit cell because such cuprates have similar Fermi energies [2–4], resistivities, anisotropies and a similar dimensionality [5–7], but exhibit a large variation of  $T_c$ . Since thermal fluctuations decrease with decreasing temperature and vanish at  $T \rightarrow 0$ , an analysis of the interplay between the pseudogap and superconductivity in very low- $T_c$  cuprates may provide an important constraint for theoretical models.

Single crystals of Bi-cuprates represent natural stacks of atomic-scale intrinsic Josephson junctions [8–11]. The  $c$ -axis transport is caused by interlayer tunneling, which creates the basis for the intrinsic tunneling spectroscopy technique and facilitates measurements of bulk electronic spectra of cuprates [12, 13].

In this work we present combined intrinsic tunneling and transport measurements of  $\text{Bi}_{2+x}\text{Sr}_{2-y}\text{CuO}_{6+\delta}$

(Bi-2201) single crystals with low  $T_c \lesssim 4$  K. We observe that all superconducting characteristics (temperature, energy and magnetic field scales) are reduced in proportion to  $T_c$ , but the corresponding pseudogap characteristics remain similar to that in high- $T_c$  Bi-2212 and Bi-2223 compounds with 20–30 times larger  $T_c$ . The disparity of the superconducting and  $c$ -axis pseudogap scales in Bi-2201 clearly reveals their different origins.

We study small mesa structures made on top of freshly cleaved Bi-2201 single crystals. The crystals were grown similar to Ref. [14]. The  $T_c$  of the crystals depends not only on oxygen doping  $\delta$ , but also on the Bi and Sr content and can be tuned to zero in the stoichiometric  $x = y = 0$  compound. As-grown crystals are slightly overdoped (OD) with a  $T_c \simeq 3.5$  K. Six or twelve mesas/contacts were fabricated on each crystal, which allows simultaneous measurements of the  $ab$ -plane and the  $c$ -axis transport characteristics in the four-probe configuration. In total about ten crystals were studied and the data shown below are representative for all samples. Most measurements were done in a flowing gas  $^4\text{He}$  cryostat at  $1.8 \text{ K} < T < 300 \text{ K}$  and a magnetic field up to 17 T, or a  $^3\text{He}$  cryostat with  $T$  down to 270 mK and a field up to 5 T. Complementary measurements were made in pulsed magnetic fields up to 65 T. In all cases magnetic field was applied along the  $c$ -axis direction.

In order to minimize self-heating in the intrinsic tunneling experiments, we limited the height of the mesas to only a few atomic layers, using slow 250 eV Ar-ion milling, as well as reduced lateral mesa sizes down to sub-micrometers, using a dual-beam SEM/FIB system for mesa patterning or trimming. Two different miniaturization techniques were used, providing slightly different mesa properties. In the first technique we initially made moderately large  $\sim 5 \times 5 \mu\text{m}^2$  mesas using optical lithog-

raphy and subsequently trimmed them to smaller sizes [9]. In the second technique we directly patterned small mesas using electron-beam deposited Pt/C masks, followed by O-plasma ashing of remaining C. Such mesas are shown in Fig. 1(a). They are completely covered by  $\sim 200$  nm thick gold electrodes, which further improve the thermal properties of the mesas.

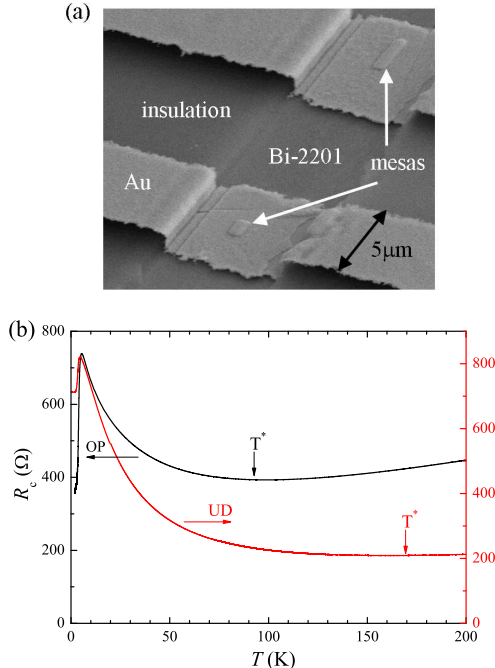


FIG. 1. (a) SEM image of Bi-2201 mesas. Sub-micron mesas were made by direct patterning of Pt masks in a dual-beam SEM/FIB. (b) Zero bias  $c$ -axis resistance for an optimally doped (OP) mesa with  $T_c \simeq 4.0$  K and for an underdoped (UD) mesa with  $T_c \simeq 3.7$  K. The pseudogap opening temperatures  $T^*$  are indicated by arrows.

The main difference between both types of mesas is in the size of the mesa being Ar-milled. Ar-milling leads to a partial out-diffusion of oxygen. The smaller the mesa area is during milling, the easier is an in-plane O-diffusion, which leads to a lower doping of the mesa after milling. Fig. 1(b) shows the zero-bias  $c$ -axis resistance  $R_c(T)$  for mesas made by those two techniques. The mesas made by the first technique show a metallic behavior at high temperatures, which turns into a semiconducting-like at  $T^* \sim 95$  K, while the mesas made by the second technique show semiconducting behavior already at  $T^* \simeq 170$  K (determined from the minimum in  $R(T)$ ). By comparing with reported doping dependences of  $R_c(T)$  for Bi-2201 [6, 15], we conclude that the former mesa is near optimally doped (OP), while the latter became slightly underdoped (UD). This is accompanied by a systematic variation of the critical temperature from  $T_c \simeq 3.5$  K for as grown overdoped crystals to  $T_c \simeq 4.0$  K (OP) and 3.7 K (UD) for mesas made by the first and second technique, respectively. The decoupling

of  $T_c$  and  $T^*$  in our low- $T_c$  Bi-2201 allows a clear analysis of the pure PG behavior above  $T_c$  without an interference from superconductivity. From Fig. 1(b) it is clear that the pseudogap  $T^*$  grows rapidly with underdoping, similar to that for La-doped Bi-2201 (Bi(La)-2201) [10, 15] and consistent with the existence of a quantum critical doping point [16].

An unambiguous discrimination of spectroscopic features from self-heating artifacts can be obtained by studying the size dependence of current-voltage ( $I$ - $V$ ) characteristics: spectroscopic features are material properties and should be size independent, while heating strongly depends on the mesa size [12, 17]. Fig. 2(a) shows intrinsic tunneling conductances  $dI/dV(V)$  at low  $T$  and  $H$  for UD mesas with different areas (from 0.8 to  $2.5 \mu\text{m}^2$ ). They are fabricated on the same crystal and the mesa conductance scales with their area. It can be seen that all curves maintain similar shapes in the semi-logarithmic scale, despite significant differences in dissipation powers (the power at the peaks is ranging between  $\approx 1.2$  and  $7.4 \mu\text{W}$ ). The size-independence indicates that there is no significant distortion by self-heating.

From Fig. 2(a) it can be seen that the intrinsic tunneling characteristics exhibit a peak-dip structure, typical for tunneling characteristics of (underdoped) cuprates [18–23]. The peak is attributed to the superconducting sum-gap singularity at  $V_{\text{peak}} = 2\Delta_{\text{SG}}N/e$ , where  $N$  is the number of stacked intrinsic junctions in the mesa [12, 13]. The dip is usually ascribed to an interaction with a collective bosonic mode with energy  $\Omega_B$ , in which case  $eV_{\text{dip}} = 2\Delta_{\text{SG}} + \Omega_B$  (per junction) [18, 19]. The ratio  $\Omega_B/2\Delta_{\text{SG}} \simeq 0.62$  can be extracted explicitly from the  $dI/dV(V)$  characteristic in Fig. 2(b). It is very close to the average value  $\simeq 0.64$ , deduced from inelastic neutron scattering data for different cuprates [24].

In order to evaluate absolute values of  $\Delta_{\text{SG}}$  and  $\Omega_B$ , we have to estimate the number of junctions  $N$  in the mesas. For high- $T_c$  Bi-2212 [8, 12] and (Bi(La)-2201) [10, 11] this is simply done by counting quasiparticle branches in the  $I$ - $V$  characteristics. However, in low- $T_c$  Bi-2201, the branches are not distinguishable [10]. Still it is possible to estimate  $N$  by comparing the peak voltages of mesas with different heights. Since the uniformity of Ar-milling is typically about one crystallographic unit cell, there is a certain probability that mesas on the same crystal have either  $N$  or  $N + 1$  junctions. In Fig. 2(a) this is seen as two series of peaks with slightly different voltages, marked by downward and upward arrows, respectively. Assuming that the ratio of voltages is  $(N + 1)/N$ , we obtain that one series of mesas contains  $N = 5$  and the other  $N = 6$  intrinsic junctions. This yields  $\Delta_{\text{SG}} \simeq 0.55 \pm 0.1$  meV and  $2\Delta/k_B T_c \simeq 3.5 \pm 0.6$ , which is typical for weak-coupling superconductors and consistent with previous studies on Bi(La)-2201 with higher  $T_c$  [10, 18, 21, 25]. The corresponding bosonic mode energy is also small,  $\Omega_B \simeq 0.7$  meV, and is clearly not related

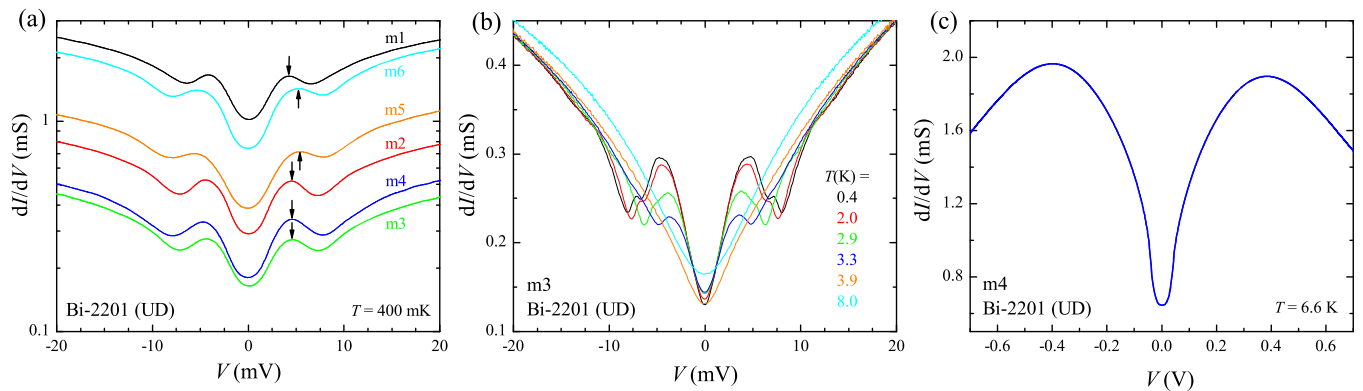


FIG. 2. (Color online) (a) Intrinsic tunneling conductances (in the semi-log scale) at 400 mK for UD mesas with different areas ( $0.8$  to  $2.5 \mu\text{m}^2$ ), fabricated on the same crystal. Downward and upward arrows mark sum-gap peaks for mesas with  $N = 5$  and  $6$  junctions, respectively. It is seen that the  $dI/dV(V)$  characteristics retain the same shape with a peak and a dip, despite a significant difference in mesa sizes and power dissipation, which indicates the lack of distortion by self-heating. (b) Temperature dependence of  $dI/dV(V)$  curves for the smallest mesa. It is seen that both the peak and dip features disappear in the BCS mean-field manner at  $T \rightarrow T_c$ . (c) A large bias  $dI/dV(V)$  at  $6.6 \text{ K}$  showing the pronounced conductance suppression caused by the  $c$ -axis pseudogap at  $T > T_c$ . Note the large scale of the pseudogap hump, which corresponds to  $\Delta_{PG} \simeq 40 \text{ meV}$ .

to the much higher phonon or antiferromagnetic energies. This observation demonstrates that  $\Omega_B$  is determined solely by  $\Delta_{SG}(T)$  and supports the interpretation of the mode as an exciton of Bogoliubov quasiparticles caused by a  $d$ -wave symmetry of the order parameter [26].

Fig. 2 (b) shows the  $T$ -dependence of  $dI/dV(V)$  characteristics for the smallest UD mesa at  $H = 0 \text{ T}$ . One can clearly see that both, the peak and the dip decrease in amplitude, move to lower voltages with increasing  $T$  and vanish at  $T_c \simeq 3.7 \text{ K}$  in the BCS mean-field manner (flat at  $T \ll T_c$  and a fast decay at  $T \rightarrow T_c$ ). Above  $T_c$ , the  $dI/dV(V)$  remains V-shaped due to the presence of the  $c$ -axis PG, which leads to thermal activation behavior of interlayer transport [12, 27]. Fig. 2 (c) shows a large bias  $dI/dV(V)$  of an UD mesa at  $T = 6.6 \text{ K} > T_c$ . The pseudogap hump is clearly visible at  $V \simeq 0.4 \text{ V}$ , corresponding to  $\Delta_{PG} \simeq 40 \text{ meV}$ . It is remarkably similar to that for Bi-2212 [10, 12, 23, 27], despite a more than 20 times smaller  $T_c$  and  $\Delta_{SG}$ . The large  $\Delta_{PG}$  leads to the high onset temperature  $T^* \sim 170 \text{ K}$  in the UD mesa, see Fig. 1 (b). Obviously, there is a large difference between the superconducting and the  $c$ -axis pseudogap energies in low- $T_c$  Bi-2201.

From Fig. 2 (b) it is clear that the thermal-activation-like [12, 27], V-shaped PG characteristics coexists with superconductivity at  $T < T_c$ . This makes it difficult to separate superconducting and pseudogap-related phenomena below  $T_c$  by looking solely on the  $T$ -variation of experimental characteristics [2]. A more unambiguous discrimination between them can be done by analyzing magnetic field effects [13]. The upper critical field  $H_{c2}$ , required to suppress spin-singlet superconductivity, is limited by the paramagnetic (Zeeman) effect. This yields  $dH_{c2}/dT(T = T_c) = -2.25 \text{ T/K}$  for weak coupling

$d$ -wave superconductors and lower values for strong coupling cases [28]. Therefore,  $H_{c2}$  for low- $T_c$  Bi-2201 should be much lower and easier accessible than for high- $T_c$  Bi-2212 with  $H_{c2} \sim 100 \text{ T}$  [13].

Fig. 3 (a) shows zero-bias  $ab$ -plane resistances,  $R_{ab}(T)$ , at different magnetic fields in the  $c$ -axis direction for the OP mesa with  $T_c(H = 0) = 4.0 \pm 0.5 \text{ K}$ . With increasing  $H$ ,  $T_c$  decreases and is no longer visible at  $H > 10 \text{ T}$ . Fig. 3 (b) shows similar data for the UD mesa, measured down to sub-Kelvin temperatures. The graph demonstrates that the  $T_c$  is indeed completely suppressed by a field of a few Tesla.

A significant positive magnetoresistance can be seen in the  $R_{ab}(T, H)$  curves in Figs. 3 (a) and (b) which persists well above  $T_c$ , indicating a broad superconducting fluctuation region. Fig. 3 (c) represents the normalized excess conductance  $[1/R_{ab}(T, H) - 1/R_n(T)]R_n(T)$  vs.  $T$  for the data from Fig. 3 (a). Here we used the curve at  $H = 14 \text{ T}$  as normal state resistance  $R_n(T) = R_{ab}(T, H = 14 \text{ T})$ . The fluctuation MR of Bi-2201 is decreasing almost exponentially with increasing  $T$ , which was also observed for Bi-2212 [13]. The MR falls to less than 1% at a relative temperature  $T/T_c(H) \simeq 2.3$ , comparable to that for Bi(La)-2201 with higher  $T_c$  [15]. Even though we can not exclude an additional influence of sample inhomogeneity on the broadening of the superconducting transition, it is clear that the temperature range of superconducting fluctuations is determined by  $T_c$  and not by the much larger  $T^* \sim 100 - 200 \text{ K}$ .

Fig. 3 (d) shows the interlayer tunneling conductance  $dI/dV(V)$  at different  $c$ -axis magnetic fields and at  $T = 400 \text{ mK}$  for a small UD mesa. Both, the peak and the dip are moving to lower voltages and smear out

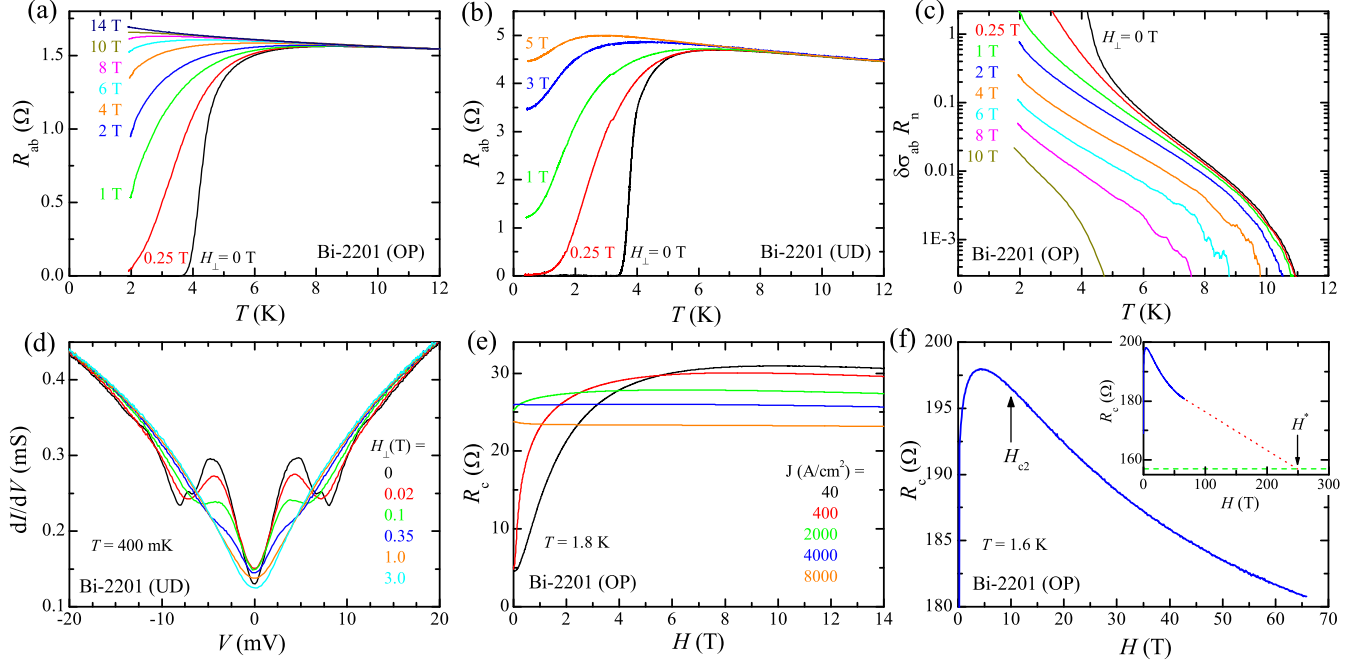


FIG. 3. (Color online) Zero-bias *ab*-plane resistance at different *c*-axis magnetic fields for (a) an OP mesa and (b) an UD mesa. A complete suppression of  $T_c$  at  $H_{c2} \simeq 10$  T is seen. (c) Normalized in-plane fluctuation (excess) conductance  $[1/R_{ab}(T, H) - 1/R_n(T)]R_n(T)$  vs.  $T$  for the data from (a). It is seen that fluctuations decay rapidly (almost exponentially) with increasing  $T$  and that the region of significant fluctuations expand to about twice the  $T_c$ . (d) Magnetic field dependence of intrinsic tunneling characteristics for an UD mesa at 400 mK. The sum-gap peak and the dip are washed away in a *c*-axis field of a few Tesla. (e) Bias current dependence of the *c*-axis tunneling magnetoresistance (MR) for an OP mesa. The MR is large at small current densities but vanishes at large bias, corresponding to the nearly ohmic normal (tunnel) resistance part of the *I-V*. (f) *c*-axis MR in a pulsed field. A profound negative MR at large fields is attributed to suppression of the pseudogap. The inset demonstrates an estimation of the PG suppression field  $H^* \sim 250 \pm 50$  T by extrapolation to a large bias,  $H$ - and  $T$ -independent tunneling resistance (dashed horizontal line).

in a correlated manner with increasing  $H$ . The tunneling MR remains significant at a bias several times larger than at the sum-gap peak, corresponding to a dissipation power about an order of magnitude larger than at the peak. This, again, indicates the absence of significant self-heating at the peak. From the combined transport, Fig. 3(a), and magnetotunneling measurements, Fig. 3(d), we estimate  $H_{c2}(0) = 10 \pm 2$  T and  $H_{c2}(0)/T_c = 2.5 \pm 1$  T/K, consistent with previous reports [5, 13, 29]. This value is close to the paramagnetic limit, which rules out a major underestimation of  $H_{c2}$ .

In Fig. 3(e) the bias dependence of the interlayer tunneling MR for a moderately large OP mesa at  $T = 1.8$  K is shown. It demonstrates that the MR has a strong bias dependence and vanishes at large bias, corresponding to the normal (tunnel) resistance part of the *I-V*, which is the consequence of state conservation [13].

Fig. 3(f) shows the zero-bias *c*-axis resistance  $R_c(H)$  of a smaller OP mesa from the same sample, measured in a pulsed magnetic field up to 65 T. Two contributions to the MR are clearly seen: At low fields there is a positive MR due to suppression of the interlayer supercurrent, as in panel (e), and at higher fields a transition to a pro-

found negative MR occurs, which does not saturate at 65 T. A very large characteristic field,  $H^* \sim 250 \pm 50$  T, is estimated by linear extrapolation to an (almost)  $H$ - and  $T$ -independent, high bias tunnel resistance (dashed horizontal line in the inset of Fig. 3(f)). Even though such behavior has been reported before [5, 6, 30], its interpretation for high- $T_c$  cuprates is complicated by a large  $H_{c2} \sim 100$  T [13]. The low- $T_c$  of our Bi-2201 leads to a complete separation of the superconducting  $H_{c2} \sim 10$  T and the pseudogap  $H^* \sim 250$  T field scales. We attribute the negative *c*-axis magnetoresistance at  $H^* \gg H_{c2}$  to a field suppression of the PG, associated either with an (antiferro-) magnetic [3, 29] or spin/charge density wave order [20].

To summarize, combined transport and intrinsic tunneling measurements were performed on a low- $T_c$  Bi-2201 cuprate. Despite the very low  $T_c \lesssim 4$  K, the *c*-axis pseudogap characteristics ( $\Delta_{PG} \simeq 40$  meV,  $T^* \sim 100 - 300$  K, and  $H^* \sim 200 - 300$  T) are remarkably similar to those for high- $T_c$  Bi-2212 and Bi-2223 compounds with 20-30 times higher  $T_c$ . On the contrary, all superconducting properties ( $2\Delta_{SG}/k_B T_c \simeq 3.5 \pm 0.6$ , the bosonic mode

$\Omega_B/k_B T_c \simeq 2.2$ ,  $H_{c2}(0)/T_c \simeq 2.5 \pm 1$  T/K and the fluctuation region are scaling down with  $T_c$ . The striking difference between the energy, temperature and magnetic-field scales, associated with superconductivity, and the pseudogap clearly reveals their different origins. Note that the observed scaling of superconducting properties with  $T_c$  is similar to that for high- $T_c$  cuprates [5, 15, 21, 24, 25, 31]. Such a universality within a homologous family of Bi-based cuprates with similar carrier concentrations, resistivities, anisotropies and layeredness, but largely different  $T_c$  suggests that the superconducting transition maintains the same character with a similar relative strength of superconducting fluctuations, irrespective of  $T_c$ .

Support by the K. & A. Wallenberg foundation, the Swedish Research Council, and the SU-Core facility in Nanotechnology is gratefully acknowledged. The high-field experiment was done with support from EuroMag-NET II under the EC Contract No. 228043. A. Maljuk thanks C. T. Lin (MPI-Stuttgart) for helpful discussions regarding the crystal growth.

---

\* E-mail: Vladimir.Krasnov@fysik.su.se

- [1] A. I. Larkin and A. A. Varlamov, *Theory of Fluctuations in Superconductors* (Oxford University Press, New York, 2009).
- [2] T. Kondo, Y. Hamaya, A. D. Palczewski, T. Takeuchi, J. S. Wen, Z. J. Xu, G. Gu, J. Schmalian and A. Kaminski, *Nature Phys.* **7**, 21 (2011).
- [3] R. H. He et al., *Science* **331**, 1579 (2011).
- [4] Y. Okada, T. Kawaguchi, M. Ohkawa, K. Ishizaka, T. Takeuchi, S. Shin and H. Ikuta *Phys. Rev. B* **83**, 104502 (2011).
- [5] S. I. Vedenev, A. G. M. Jansen, E. Haanappel and P. Wyder, *Phys. Rev. B* **60**, 12467 (1999).
- [6] Y. Ando, G. S. Boebinger, A. Passner, N. L. Wang, C. Geibel, and F. Steglich, *Phys. Rev. Lett.* **77**, 2065 (1996).
- [7] T. Watanabe, T. Fujii, and A. Matsuda, *Phys. Rev. Lett.* **79**, 2113 (1997).
- [8] R. Kleiner and P. Müller, *Phys. Rev. B* **49** 1327 (1994).
- [9] S. O. Katterwe and V. M. Krasnov, *Phys. Rev. B* **80**, 020502(R) (2009).
- [10] A. Yurgens, D. Winkler, T. Claeson, S. Ono and Y. Ando *Phys. Rev. Lett.* **90**, 147005 (2003).
- [11] H. Kashiwaya, T. Matsumoto, H. Shibata, H. Eisaki, Y. Yoshida, H. Kambara, S. Kawabata and S. Kashiwaya, *Appl. Phys. Express* **3**, 043101 (2010).
- [12] V. M. Krasnov, *Phys. Rev. B* **79**, 214510 (2009).
- [13] V. M. Krasnov, H. Motzkau, T. Golod, A. Rydh, S. O. Katterwe and A. B. Kulakov *Phys. Rev. B* **84**, 054516 (2011).
- [14] B. Liang, A. Maljuk and C. T. Lin, *Physica C* **361**, 156 (2001).
- [15] A. N. Lavrov, Y. Ando and S. Ono, *Europhys. Lett.* **57**, 267 (2002).
- [16] F. F. Balakirev, J. B. Betts, A. Migliori, I. Tsukada, Y. Ando and G. S. Boebinger, *Phys. Rev. Lett.* **102**, 017004 (2009).
- [17] V. M. Krasnov, M. Sandberg and I. Zogaj, *Phys. Rev. Lett.* **94**, 077003 (2005).
- [18] N. Miyakawa, J. F. Zasadzinski, S. Oonuki, M. Asano, D. Henmi, T. Kaneko, L. Ozyuzer and K. E. Gray, *Physica C* **364-365**, 475 (2001).
- [19] G. L. de Castro, Ch. Berthod, A. Piriou, E. Giannini and Ø. Fischer, *Phys. Rev. Lett.* **101**, 267004 (2008).
- [20] W. D. Wise, M. C. Boyer, K. Chatterjee, T. Kondo, T. Takeuchi, H. Ikuta, Y. Wang and E. W. Hudson *Nature Phys.* **4**, 696 (2008).
- [21] T. Kato, H. Funahashi, H. Nakamura, M. Fujimoto, T. Machida, H. Sakata, S. Nakao and T. Hasegawa, *J. Supercond. Nov. Magn.* **23**, 771 (2010).
- [22] M. Kugler, Ø. Fischer, Ch. Renner, S. Ono and Y. Ando, *Phys. Rev. Lett.* **86**, 4911 (2001).
- [23] V. M. Krasnov, *Phys. Rev. B* **65**, 140504(R) (2002).
- [24] G. Yu, Y. Li, E. M. Motoyama and M. Greven *Nature Phys.* **5**, 873 (2009).
- [25] S. Ideta et al., *arXiv*: **1104.0313**.
- [26] Z. Hao and A. V. Chubukov, *Phys. Rev. B* **79**, 224513 (2009).
- [27] S. O. Katterwe, A. Rydh and V. M. Krasnov, *Phys. Rev. Lett.* **101**, 087003 (2008).
- [28] J. P. Carbotte, *Rev. Mod. Phys.* **62**, 1027 (1990).
- [29] S. Kawasaki, C. Lin, P. L. Kuhns, A. P. Reyes, and G. Q. Zheng, *Phys. Rev. Lett.* **105**, 137002 (2010).
- [30] T. Kawakami, T. Shibauchi, Y. Terao, M. Suzuki, and L. Krusin-Elbaum, *Phys. Rev. Lett.* **95**, 017001 (2005).
- [31] A. Dubroka et al., *Phys. Rev. Lett.* **106**, 047006 (2011).